Journal of Visualized Experiments
Applying the RatWalker System for Gait Analysis in a Genetic Rat Model of Parkinson's Disease
--Manuscript Draft--

Article Type:	Invited Methods Article - JoVE Produced Video
Manuscript Number:	JoVE62002R2
Full Title:	Applying the RatWalker System for Gait Analysis in a Genetic Rat Model of Parkinson's Disease
Corresponding Author:	Kelly Stauch, Ph.D. University of Nebraska Medical Center Omaha, NE UNITED STATES
Corresponding Author's Institution:	University of Nebraska Medical Center
Corresponding Author E-Mail:	kelly.stauch@unmc.edu
Order of Authors:	Kelly Stauch, Ph.D.
	Steven Totusek
	Trey Farmer
	Benjamin Lamberty
	Kelsey Dyball
	Mohannad Almikhlafi
	Howard Fox

Additional Information:	
Question	Response
Please specify the section of the submitted manuscript.	Neuroscience
Please indicate whether this article will be Standard Access or Open Access.	Standard Access (US$2,400)
Please indicate the **city, state/province, and country** where this article will be **filmed**. Please do not use abbreviations.	Omaha, NE, USA
Please confirm that you have read and agree to the terms and conditions of the author license agreement that applies below:	I agree to the Author License Agreement
Please provide any comments to the journal here.	

1 **TITLE:**
2 **Applying the RatWalker System for Gait Analysis in a Genetic Rat Model of Parkinson's Disease**
3
4 **AUTHORS AND AFFILIATIONS:**
5 Kelly L. Stauch[1], Steven Totusek[1], Trey Farmer[1], Benjamin G. Lamberty[1], Kelsey N. Dyball[1],
6 Mohannad A. Almikhlafi[1], Howard S. Fox[1]
7
8 [1]Department of Neurological Sciences, University of Nebraska Medical Center, Omaha, NE
9
10 **Corresponding Author:**
11 Kelly L. Stauch (kelly.stauch@unmc.edu)
12
13 **Co-Authors:**
14 Steven Totusek (steven.totusek@unmc.edu)
15 Trey Farmer (trey.farmer@unmc.edu)
16 Benjamin G. Lamberty (bglamberty@unmc.edu)
17 Kelsey N. Dyball (Kelsey.dyball@unmc.edu)
18 Mohannad A. Almikhlafi (mohannad.almikhlafi@unmc.edu)
19 Howard S. Fox (hfox@unmc.edu)
20
21 **KEYWORDS:**
22 Locomotor, Gait analysis, Parkinson's disease, Parkin, Pink1
23
24 **SUMMARY:**
25 Here we describe the RatWalker system, built by redesigning the MouseWalker apparatus to
26 accommodate for the increased size and weight of rats. This system uses frustrated total internal
27 reflection (FTIR), high-speed video capture, and open-access analysis software to track and
28 quantify gait parameters.
29
30 **ABSTRACT:**
31 Parkinson's disease (PD) is a progressive neurodegenerative disorder caused by the loss of
32 dopaminergic (DA) neurons in the substantia nigra pars compacta. Gait abnormalities, including
33 decreased arm swing, slower walking speed, and shorter steps are common in PD patients and
34 appear early in the course of disease. Thus, the quantification of motor patterns in animal models
35 of PD will be important for phenotypic characterization during disease course and upon
36 therapeutic treatment. Most cases of PD are idiopathic; however, the identification of hereditary
37 forms of PD uncovered gene mutations and variants, such as loss-of-function mutations in Pink1
38 and Parkin, two proteins involved in mitochondrial quality control that could be harnessed to
39 create animal models. While mice are resistant to neurodegeneration upon loss of Pink1 and
40 Parkin (single and combined deletion), in rats, Pink1 but not Parkin deficiency leads to nigral DA
41 neuron loss and motor impairment. Here, we report the utility of FTIR imaging to uncover gait
42 changes in freely walking young (2 months of age) male rats with combined loss of Pink1 and
43 Parkin prior to the development of gross visually apparent motor abnormality as these rats age
44 (observed at 4-6 months), characterized by hindlimb dragging as previously reported in Pink1

45   knockout (KO) rats.

46

47   **INTRODUCTION:**

48   PD, the most common age-related neurodegenerative movement disorder, is caused by the loss
49   of DA neurons in the substantia nigra pars compacta. This loss of nigral DA neurons and the DA
50   inputs into the striatum lead to the observed motor function impairments seen in patients with
51   PD[1,2]. The defining motor characteristics of patients with PD, known collectively as Parkinsonism,
52   include rigidity, resting tremor, bradykinesia, postural instability, and micrographia[3].
53   Furthermore, gait disturbances, which are common in PD patients, appear early in the course of
54   disease[1,4,5]. While certain lifestyles are suggested to help slow the progression of PD, such as
55   healthy eating and regular exercise, there is currently no cure for PD, only medications to manage
56   the symptoms. This leaves room for the need of further investigation in hopes of improved
57   therapeutics. Thus, characterization of the gait pattern in PD animal models is a crucial tool to
58   characterize the relevance of the model as well as how therapeutic treatments aimed at
59   controlling PD are preventing or improving motor impairments.

60

61   There are various PD animal models that have been used to test therapeutic treatments, however
62   each one has their limitations. For example, animal models treated with the neurotoxin 1-methyl-
63   4-phenyl-1,2,3,6-tetrahydropyridine (MPTP) have yielded a great wealth of information about
64   processes important for nigral DA neuron loss and subsequent striatal adaptations, and pointed
65   to the role of mitochondria in PD pathogenesis; however, the pathogenetic background of the
66   MPTP model is of a toxic nature rather than a neurodegenerative process as in human PD[6].
67   Additional chemically inducible models include 6-hydroxydopamine (6-OHDA) and rotenone. 6-
68   OHDA was the first agent used to induce PD by selective accumulation of the drug in the DA
69   neurons, which eventually kills the neurons and leads to PD like symptoms. This model was first
70   used for the tracking of DA depletion by examining the behavior in response to amphetamine
71   and apomorphine[7]. This method of PD induction has proved to be useful for the screening of
72   pharmacological agents that impact DA and its receptors[8]. While the 6-OHDA model is a great
73   model for tracking quantifiable motor deficits, this model does not show how the gradual loss of
74   neurons and formation of Lewy bodies impact the animal. The other method of induction,
75   rotenone, has been shown to have progressive degeneration of nigrostriatal neurons with the
76   loss of tyrosine hydroxylase and DA transporter, allowing for a better model to track loss of
77   neurons over time[9]. The rotenone treated rats showed bradykinesia, postural instability, and
78   unsteady gait[10]. However, this method has been found to be widely variable between different
79   strains of rats, which has provoked questioning whether or not rotenone is a reliable PD model[11-
80   13]. While gait analysis has been shown to be impacted by the induction of PD in rats, to date,
81   genetically induced PD rat models have not been readily used for gait analysis by freely walking
82   down a runway.

83

84   One way to analyze motor impairment in freely walking rodents is kinematic gait analysis, which
85   can be performed by utilizing FTIR imaging. This established method uses an optical touch sensor
86   based on FTIR, which records and tracks the footprints of the rodents as they move down the
87   runway[14-16]. As compared to other methods, FTIR does not depend on any markers on the
88   animal's body that could interfere with the paw prints. Generation of the video data produces

89   digital paw prints of all four limbs that can be combined to create a dynamic and reproducible
90   walking pattern for various rodent models. The principle of imaging-based gait analysis is to take
91   each individual paw and measure the contact area over time as the rodent walks down the
92   runway. Each stance is represented by an increase in paw area (in the braking phase) and a
93   decrease in paw area (in the propulsion phase). This is proceeded by the swing phase, which is
94   when there is no paw signal detected. After evaluation of the video, several parameters are
95   generated that can be used to compare wild-type (WT) versus PD model. Some examples of the
96   parameters are step length (distance the paw covers in one step), swing duration (duration of
97   time the paw is not in contact with the runway), swing speed (step length as a function of swing
98   duration), and step pattern (diagonal steps, lateral steps, or girdle steps).
99
100 To demonstrate the utility of FTIR to uncover early gait pattern changes in rats, we used a genetic
101 rat model of PD. While most cases of PD are idiopathic; the identification of hereditary forms of
102 PD uncovered gene mutations and variants, such as loss-of-function mutations in Pink1 and
103 Parkin, two proteins involved in mitochondrial quality control[17], that could be harnessed to
104 create animal models[18]. Unfortunately, mice are resistant to neurodegeneration upon loss of
105 these proteins (single and combined)[19-21]. In rats, Pink1 but not Parkin deficiency leads to nigral
106 DA neuron loss and motor impairments[22], but without complete penetrance. Therefore, we
107 generated a combined Pink1/Parkin double knockout (DKO) rat model, which displays the overt
108 visually apparent hindlimb dragging phenotype reported in male Pink1 KO rats[22] but now at a
109 higher rate: 100% versus 30-50% of males between 4-6 months.
110
111 While this method works well for analyzing motor deficits in mice[14], FTIR imaging gait system
112 specifications to accommodate the size and weight of rats was previously unavailable
113 noncommercially. Here we explain how to build the RatWalker, a modified FTIR gait imaging
114 system modeled after the MouseWalker[14], except adapted for the size and weight of rats. This
115 system utilizes an optical effect, FTIR, to provide a method to visualize and subsequently record
116 animal footprints for analysis. Contact of an animal's foot with the optical waveguide (platform)
117 causes disruption in the light path resulting in a visible scattering effect, which is captured using
118 domestic-grade, high-speed videography and processing using open-source software. This study
119 demonstrates the power of FTIR imaging in studying gait changes in genetic rat models of PD. For
120 example, while overt visually apparent motor changes (i.e. hindlimb dragging) are observed in
121 male DKO rats at 4 months at the earliest, using FTIR we are able to uncover gate abnormalities
122 in male DKO rats at 2 months of age.
123
124 **PROTOCOL:**
125
126 All animal studies were approved by the University of Nebraska Medical Center Institutional
127 Animal Care and Use Committee (IACUC).
128
129 1.   **Gait apparatus**
130
131 NOTE: Modeled from the MouseWalker[14], the RatWalker was designed with dimensions in
132 proportion to the difference in step length between rats and mice. It consists of a side

illumination backlight, walkway enclosure, optical waveguide walkway, mirror, and camera (**Figure S1**). LED strips, oriented in a staggered position, were used on each side of the walkway and backlight waveguides to accommodate the extra material. The materials needed to build the modified gait apparatus can be found in **Table S1**.

1.1.   Use a backlight (**Figure S2**) to create a silhouette of the animal which is utilized by the software to assign position, direction of movement, and morphometric qualities. Construction is comprised of a layered panel of an acrylic diffuser, optical waveguide, reflector, and LED light strips assembled within a stock aluminum frame (**Table S1**).

1.2.   Use a walkway enclosure (**Figure S3**) to guide the animal along the platform and direct the animal to the home-cage. Construction consists of clear acrylic sheets solvent welded with dichloromethane (**Table S2**).

1.3.   Use the walkway (**Figure S4**) to provide the medium to generate lit footprints. The walkway is constructed from clear acrylic, which is side-lit with strip LEDs and housed in aluminum angle (**Table S3**).

1.4.   Place a mirror (**Figure S5**) directly under the walkway at a 45-degree angle to reflect the underside of the walkway for videography. It is constructed from a 1/4" thick glass mirror supported by acrylic, and angled brackets arranged in a row (**Table S4**).

1.5.   Perform videography using a tripod-mounted, domestic-quality, high-speed action camera.

2.   Equipment Setup

2.1.   Align the backlight, walkway, and mirror according to **Figure S1**, on top of a countertop, workbench, or stable cart. Ensure each component is centered with respect to the walkway.

2.2.   Using a level, make certain that the components are horizontally plumb.

2.3.   Place the walkway enclosure on top of the walkway.

2.4.   Clean all contact surface areas with 70% ethanol. Make sure to use a nonabrasive towel to prevent scratching of the walkway.

2.5.   Mount the high-speed camera onto a 57-inch tripod and place it mid-line to the mirror, spaced far enough to capture the entire walkway inside of the field of view. From the video settings menu, ensure that the high-speed camera is set to linear acquisition in 1080p mode at 120 frames per second (fps) with any type of auto-adjust or optimizations turned off.

2.6.   Plug in and turn on the LED strip lights for the backlight and walkway. It may be necessary to dim the backlight to reduce background capture.

177
178   3.   **Animal Acclimation**
179
180   NOTE: One week prior to the first experiment, run the animals through the modified gait
181   apparatus.
182
183   3.1.   Position a home-cage at the terminus of the walkway.
184
185   3.2.   With the enclosure installed and the lights off, place the rat at the end of walkway
186   opposite the home-cage and allow it to walk across the walkway in an unforced manner.
187
188   3.3.   Run each rat through the modified gait apparatus several times, until they can smoothly
189   cross the entire walkway.
190
191   3.4.   Repeat the process two days before the experiment.
192
193   4.   **Gait Procedure**
194
195   4.1.   Place a home-cage at the end of the walkway before the start of each run to serve as a
196   positive cue for the rat to traverse the walkway.
197
198   4.2.   Turn off the room lights, power on the camera, and start recording several seconds before
199   the rat is placed on the platform.
200
201   NOTE: Be certain to use a memory card that is officially recommended by the camera
202   manufacturer. An unlisted memory card may still work but is not guaranteed to capture at the
203   purported frame rate.
204
205   4.3.   With the enclosure installed, place the rat at the end of the walkway opposite the home-
206   cage and allow it to walk across the walkway in an unforced manner.
207
208   4.4.   Stop recording once the animal reaches the terminus of the walkway.
209
210   4.5.   Clean the walkway using 70% ethanol and a nonabrasive towel in between runs and after
211   an animal urinates or defecates, then allow ethanol to evaporate before introducing another
212   animal.
213
214   4.6.   Run the rats through the walkway a total of 7 times during each observation period, taking
215   the first three runs that score as passing for analysis.
216
217   4.7.   Score a run as passing if the animal makes four or more consecutive steps in the direction
218   of the home-cage without interruption due to grooming, pausing, or errant movements.
219

5.   **Video preprocessing**

NOTE: The videos captured by the high-speed camera are rendered in mp4 format at 120 fps and a resolution of 1080p. To ease the burden on the analytical software downstream, first trim unnecessary footage and strip the audio from each video using LosslessCut software (version 3.23.7, https://github.com/mifi/lossless-cut), then convert the mp4 video stream into a png image sequence using the open-source software FFmpeg (version 4.2, http://ffmpeg.org/). Note: other Lossless formats such as tiff can be utilized in place of png.

5.1.   Create a directory for the videos on a PC running Windows 7 or higher, then transfer the videos from the high-speed camera's storage device to the newly created directory. In addition, copy ffmpeg.exe to the same location.

5.2.   In LosslessCut, drag the videos to the interface to open. Discard the audio, set the start and end cut points to include only the analytically relevant portion of the video, set the capture frame format to png, and export. Once the video is exported, rename the video file using any naming convention followed by "_trimmed".

5.3.   To batch convert the videos to image sequences, open a command prompt, set the working directory to the location of the videos with "cd [path to directory]", and run the following commands:
for %i in (*) do mkdir "%~ni_cropped"
for %i in (*) do mkdir "%~ni_trimmed"
for /f "tokens=1 delims=." %a in ('dir /B *_trimmed.MP4') do ffmpeg -i "%a.MP4" "%a/%a_%04d.png"

5.4.   After the batch process completes, open each image sequence in ImageJ Fiji[23] and crop the sequence to the region of interest (ROI) encompassing the area of the floor within which the rat is observed.

5.5.   To reduce background from the walkway illumination, increase the color balance minimum of the cyan channel to 76.

5.6.   Save as image sequence and change the "_trimmed" suffix to "_cropped", saving the files in their respective "_cropped" folder.

6.   **Gait Processing**

NOTE: Gait data is processed and quantified using the freely available software, MouseWalker

264   (http://biooptics.markalab.org/MouseWalker/)[14].

265

266   6.1.   Unpack and install the MouseWalker software onto a PC running a 64-bit windows
267   environment with Microsoft Excel installed.

268

269   6.2.   After launching MouseWalker.exe, perform an initial scale calibration for each set of runs.
270   Load an image sequence and using landmarks or a ruler captured in the video, measure two
271   points of known distance. Calculate the number of pixels per centimeter in the video frame and
272   enter this value into the parameters section of the settings form along with the video acquisition
273   frame rate.

274

275   6.3.   Similarly, measure the head, tail, and feet of the rat to determine head length, maximum
276   tail width and area, minimum and maximum foot area, and other features necessary to complete
277   the tracking parameters section of the MouseWalker settings form. See
278   http://biooptics.markalab.org/MouseWalker/ for the user manual and other documentation.

279

280   6.4.   To obtain the body area values, open the same image sequence in ImageJ, draw a
281   selection outlining the rat, and perform a region of interest (ROI) pixel count.

282

283   6.5.   Parameters and settings used for this publication (**Figure S6**).

284

285   NOTE: Parameters are provided for illustration and are dependent on the scale of the video,
286   acquisition hardware, and conditions. Software calibration and adjustment is required each time
287   the camera or equipment is re-positioned. Capturing a measuring device within the acquisition
288   improves accuracy and facilitates calibration.

289

290   6.6.   Following calibration, load each image sequence. Selecting auto will start the
291   autonomous assignment of footprints.

292

293   6.7.   Scroll through each frame of the sequence, manually correcting miss-assigned footprints.
294   Save once this step is complete.

295

296   6.8.   Lastly, select evaluate to process the footprint position and pressure data. A series of
297   graphs, images, and a spreadsheet with quantitative gait metrics will export into a results folder.

298

299   7.   **Data Analysis**

300

301   7.1.   Use the spreadsheet exported at the end of each evaluation that contains quantitative
302   gait data for each run. Concatenate data from each run and average per rat. Plot the mean data
303   and test for significance using GraphPad Prism version 7.0a.

304

305   **REPRESENTATIVE RESULTS:**
306   **Rat Colony Maintenance**
307   The generation and characterization of Pink1 and Parkin single KO rats has been described

308 previously[22]. The Pink1 and Parkin single KO rats were obtained from SAGE Labs (and now
309 available from Envigo). DKO rats were generated by crossing Pink1$^{-/-}$ rats with Parkin$^{-/-}$ rats to
310 obtain Pink1$^{+/-}$/Parkin$^{+/-}$ rats, which were interbred to obtain Pink1$^{-/-}$/Parkin$^{-/-}$ rats (will be
311 available from Envigo). To confirm the deletion of 26 bp in *Park6* (gene encoding Pink1),
312 genotyping was performed using 5'-CCCTGGCTGACTATCCTGAC-3' forward and 5'-
313 CCACCACCCACTACCACTTACT-3' reverse primers. Deletion of 5 bp in *Park2* (gene encoding Parkin)
314 was tested after DNA was amplified using a forward 5'-GGTGTCTTGGCTCAGTGTGA-3' and
315 reverse 5'-GCCACCCAGAATAGCATCTC-3'. Amplified Polymerase Chain Reaction (PCR) samples
316 were sent to ACGT Inc (Wheeling, IL) for sequencing (**Figure S7**). All rats were kept on the Long
317 Evans Hooded (LEH) background. DKO rats were viable and fertile; however, a high death rate of
318 dams during childbirth was observed (approximately 30%). Only male rats were utilized in these
319 experiments. Rats were kept in a temperature-controlled environment with a 12-hour light/dark
320 cycle and free access to rat chow and water.
321
322 **Outcomes**
323 To serve as an example of the utility of the FTIR gait analysis system for rats, adapted from[14], we
324 performed gait analysis on male WT and Pink1/Parkin DKO rats at 2 months of age to determine
325 if the use of kinematic gait analysis could uncover subtle motor impairments not observed with
326 human visual perception prior to the appearance of gross motor problems starting at 4 months
327 of age.
328
329 Similar to previous gait studies in mice[14], the adapted FTIR system was able to display the
330 footprint pattern created by the walking rat as well as the path created by the body center (**Figure
331 1A**). Despite the increased weight of the DKO rats as compared to WT (**Figure 1B**), the foot
332 pressure applied to the walking surface (visualized as heat maps) as determined by the intensities
333 of the FTIR signal, was unaltered (**Figure 1C**). Upon assessment of several gait parameters as a
334 function of walking speed (**Figure 1D-H**), we observed that the walking speed and step lengths
335 were similar between WT and DKO rats (**Figure 1D**). However, the variation between WT and
336 DKO rats became apparent in stance phase and swing duration at slower walking speeds (**Figure
337 1E, F**). The fraction of the step cycle where the leg is in the stance phase (stance duration / period)
338 is the duty factor, and this parameter highlights more time spent in the swing phase than in the
339 stance phase as the duty factor decreases, typical of running (**Figure 1G**). Again, differences are
340 highlighted at lower speeds. Further, while swing speeds increase with increased speed in WT
341 animals, the correlation is blunted in DKO rats (**Figure 1H**).
342
343 The FTIR gait analysis also allowed for plots of stance phase traces of each leg relative to the body
344 in freely walking rats (**Figure 2A, B**). The stance traces are normalized to body length and are
345 defined as the position of the foot relative to the body center from paw touchdown (anterior
346 extreme position, AEP) to the end of the stance phase (posterior extreme position, PEP). Upon
347 comparing the paw positioning, we observed significant changes in AEP (left hindlimb) and PEP
348 (right hindlimb) suggesting the left hindlimb is closer to the body during paw touchdown (AEP),
349 while the right hindlimb is further away from the body during paw takeoff (PEP) in DKO as
350 compared to WT rats (**Figure 2C**).
351

352 Several additional parameters were significantly changed in the DKO rats as compared to WT. In
353 particular, changes in hindlimb swing patterns were uncovered. The swing speed of both the left
354 and right hindlimbs was increased in DKO rats as compared to WT rats (**Figure 3A**), while the
355 swing duration of both left and right hindlimbs was decreased (**Figure 3B**). Of note, step length
356 was unaltered (**Figure 4**).
357
358 **FIGURE AND TABLE LEGENDS:**
359 **Figure 1. Footprint pattern and step parameter analysis.** Representative footprint patterns for
360 (A) WT and (B) DKO rats showing (top panel) footprint heat map representing pixel intensity and
361 horizontal line representing the body path as well as (bottom panel) individual feet labeled with
362 different colors: left fore (LF, yellow), left hind (LH, blue), right fore (RF, orange), and right hind
363 (RH, green). (C) Average walking speed for each WT (n = 7) and DKO (n = 8) rat. Mean with SEM.
364 Not significant. (D-H) Step parameters as a function of speed in WT (n = 7) and DKO (n = 8) rats.
365 Linear regression lines and R square values included. (D) Step length increases with speed in WT
366 and DKO rats. (E) Swing duration is inversely proportional to speed in WT rats, but not in DKO
367 rats (R not significant). (F) Stance duration decreases with speed in WT and DKO rats. (G) Duty
368 factor is inversely proportional to speed in DKO rats, but not WT rats (R not significant). (H) Swing
369 speed increases linearly with speed in WT rats, but not DKO rats (R not significant).
370
371 **Figure 2. Stance traces and paw positioning analysis.** (A) Representative walking track analysis
372 for a WT rat (before and after background correction) visualized with nose (red solid), head
373 contour (blue dashed), tail contour (green dashed), body center (white dashed), and footprints
374 (circles: green, RF and light blue, LH). (B) Representative plots of stance traces for freely walking
375 WT and DKO rats. (C) Paw positioning in WT (n = 7) and DKO (n = 8) rats are shown. AEP, anterior
376 extreme position; PEP, posterior extreme position; L, left; R, right; F, forepaw; H, hindpaw. Mean
377 with SEM. Significant compared to WT ($p < 0.05^*$, 0.001^{***}) using two-way ANOVA and Sidak's
378 multiple comparison test.
379
380 **Figure 3. Hindpaw swing parameters altered in DKO rats.** Forepaw and hindpaw measurements
381 of the (A) speed at which paws are moving and the (B) time paws are airborne in WT (n = 7) and
382 DKO (n = 8) rats. L, left; R, right; F, forepaw; H, hindpaw. Mean with SEM. Significant compared
383 to WT ($p < 0.01^{**}$) using Student's unpaired two-tailed t-test with Welch's correction.
384
385 **Figure 4. Step length unaltered in DKO rats.** Forepaw and hindpaw measurements of the step
386 length in WT (n = 7) and DKO (n = 8) rats. L, left; R, right; F, forepaw; H, hindpaw. Mean with SEM.
387 Significant compared to WT (not significant) using Student's unpaired two-tailed t-test with
388 Welch's correction.
389
390 **DISCUSSION:**
391 Gait disturbances, including decreased arm swing, slower walking speed, and shorter steps, are
392 a defining feature of PD, and occur early during disease course[1,5]. Several methods have been
393 developed over the years to observe and record footfalls for gait analysis in rodent models of PD,
394 with manual techniques for quantifying footfall position leading to automated approaches that
395 are more sensitive and capable of capturing dynamic parameters. Some static approaches involve

396   "inking" rodent's paws with an indicator to be tracked onto media placed on a walkway[24,25,26].
397   The residual footfalls are later quantified by hand. These methods are often used in conjunction
398   with videotaping for manual kinematic scoring. Autonomous methods of capturing and
399   quantifying gait patterns were introduced more recently[15,16], and are available commercially.
400   Autonomous gait quantification adds temporal attributes to otherwise static footprints, allowing
401   investigators to look for abnormalities attributed to velocity and time in addition to distance and
402   angle[27]. Pressure is also quantifiable when coupled with the FTIR method.

404   Gait pattern abnormalities have also been reported in toxin-induced rat models of PD. In
405   particular, gait changes have been reported in the 6-OHDA lesion model using a commercial gait
406   analysis platform[28-30]. The most prominent alteration in this model has been declines in walking
407   speed and cadence. Further, the commercial gait analysis platform has been used to assess a
408   number of dynamic and static gait parameters of PD models, such as the impact of unilateral 6-
409   OHDA-induced lesions and how transplantation of dopaminergic neurons rescues the gait
410   alterations[31]. Additionally, a study has analyzed the ratio of parameters from 6-OHDA lesions in
411   injured versus uninjured sides of the brain, while correcting for speed in related parameters such
412   as hindlimb step cycle, hindlimb print area, and step sequence, all of which are significantly
413   altered when comparing different types of lesions to saline controls[32]. However, it is important
414   to note that the pathogenetic background of toxin-induced models is of a toxic nature rather
415   than a neurodegenerative process as in human PD[6], and as such gait assessment following lesion
416   induction might mimic advanced PD when neurons are lost but make studies into early motor
417   changes more difficult.

419   Gait geometry has been measured in Pink1 KO, Parkin KO, and DJ-1 KO rats[22], models of
420   hereditary PD, that exhibit a progressive nigral dopaminergic neuron loss with aging. Gait was
421   measured using the commercial NeuroCube apparatus, where the rats are allowed to walk in a
422   circle, looking at geometry and dynamic features. Pink1 and DJ-1 KO rats showed shorter duration
423   in stride, swing, and stance when compared to WT at 4 and 8 months.

425   Because commercial gait analysis systems are costly and come with proprietary analysis
426   pipelines, we sought an open alternative for our study of hereditary rat models of PD. The
427   MouseWalker system[14], which comes with build instructions and open-access software, captures
428   all of the parameters of commercial equipment designed for small rodents. Since the platform
429   was too small to consistently achieve passable results with adult rats, i.e. four uninterrupted
430   steps during locomotion at walking speed, we re-scaled the hardware to accommodate rats. In
431   addition, we utilized a domestic action camera in place of a commercial high-speed video
432   solution.

434   Lower frame density was a potential pitfall of using an action camera in place of a high-speed
435   camera. However, the quality threshold in domestic videography is rapidly rising and is capable
436   of recording at 120 fps in high resolution. Furthermore, lens distortion can be corrected during
437   recording by camera software producing a consistently linear field of view (FOV).

439   We were initially concerned about the pressure dynamics of using a similar thickness of acrylic

440 for the walkway with a wider base and heavier animals, and the ability of the software to process
441 video of larger animals in a wider FOV. We speculate that the range of mass between mice and
442 rats falls within the range of sensitivity of the acrylic FTIR platform allowing us to measure rats
443 during their entire life cycle. Furthermore, it is possible that potential pixel dilution may be offset
444 by the higher surface area of the rats' pawprints relative to the area captured in the FOV, if there
445 is any significant difference at all. With proper calibration, as documented here, the freely
446 available software[14] was able to process rat gait video as described.

447

448 With this protocol, we were able to demonstrate that the FTIR mouse gait system[14] modified
449 here for rats can detect alterations in gait prior to the visual observation of hindlimb dragging in
450 male DKO rats. Of note, the overt visually apparent motor impairment (hindlimb dragging)
451 observed in DKO rats has been previously reported in male Pink1 single KO rats[22]. While male
452 DKO rats exhibit visually observable hindlimb dragging starting at 4-6 months of age, the gait
453 analysis uncovered locomotion changes at 2 months of age. In particular, changes in hindlimb
454 gait parameters were found. DKO rats exhibit increased hindlimb (both left and right) swing
455 speed and an associated decrease in hindlimb (both left and right) swing duration. Further, the
456 DKO rats place their left hindpaw closer to their body during paw touchdown, while the right
457 hindpaw is further away from their body during paw takeoff. While we did not uncover changes
458 in stride or stance duration in DKO rats at 2 months, the swing duration was shorter in DKO rats
459 as is similarly reported in Pink1 and DJ-1 KO rats[22]. Overall, these changes suggest the hindlimb
460 gait parameters are altered prior to the development of hindlimb dragging in male DKO rats.
461 Future longitudinal gait studies tracking the development of locomotion alterations will help
462 pinpoint the age at which gait changes become significant.

463

464 In this study, we showed that a FTIR mouse gait system[14] modified here for the study of rats can
465 be used to distinguish changes in gait parameters in 2-month-old male DKO rats, a model for
466 hereditary PD, as compared to age-matched WT rats. Previous studies in PD patients revealed
467 reduced stride length and lower average swing time, as well as increased stride time variability
468 and swing time variability[4]. Thus, our findings of changes in swing time in DKO rats, and previous
469 reports of swing time alterations in Pink1 KO and DJ-1 KO rats[22], appear relevant to PD
470 progression.

471

475

476 **DISCLOSURES:**
477 The authors declare no competing financial interests.

478

479 **REFERENCES:**
480 1   Behari, M. et al. Parkinson's disease. *Annals of Indian Academy of Neurology.* **14** (Suppl
481   1), S2-6 (2011).
482 2   Kalia, L. V., Lang, A. E. Parkinson's disease. *Lancet.* **386** (9996), 896-912 (2015).
483 3   Fahn, S. Description of Parkinson's disease as a clinical syndrome. *Annals of the New York*

484   *Academy of Sciences.* **991**, 1-14 (2003).

485   4   Frenkel-Toledo, S. et al. Effect of gait speed on gait rhythmicity in Parkinson's disease:
486   variability of stride time and swing time respond differently. *Journal of NeuroEngineering*
487   *and Rehabilitation.* **2**, 23 (2005).

488   5   Shulman, J. M., De Jager, P. L., Feany, M. B. Parkinson's disease: genetics and
489   pathogenesis. *Annual Review of Pathology.* **6**, 193-222 (2011).

490   6   Klemann, C., Martens, G. J. M., Poelmans, G., Visser, J. E. Validity of the MPTP-Treated
491   Mouse as a Model for Parkinson's Disease. *Molecular Neurobiology.* **53** (3), 1625-1636
492   (2016).

493   7   Ungerstedt, U. Striatal dopamine release after amphetamine or nerve degeneration
494   revealed by rotational behaviour. *Acta Physiologica Scandinavian Supplementum.* **367** 49-
495   68 (1971).

496   8   Beal, M. F. Experimental models of Parkinson's disease. *Nature Reviews Neuroscience.* **2**
497   (5), 325-334 (2001).

498   9   Betarbet, R. et al. Chronic systemic pesticide exposure reproduces features of Parkinson's
499   disease. *Nature Neuroscience.* **3** (12), 1301-1306 (2000).

500   10 Cannon, J. R. et al. A highly reproducible rotenone model of Parkinson's disease.
501   *Neurobiology of Disease.* **34** (2), 279-290 (2009).

502   11 Ouary, S. et al. Major strain differences in response to chronic systemic administration of
503   the mitochondrial toxin 3-nitropropionic acid in rats: implications for neuroprotection
504   studies. *Neuroscience.* **97** (3), 521-530 (2000).

505   12 Cicchetti, F., Drouin-Ouellet, J., Gross, R. E. Environmental toxins and Parkinson's disease:
506   what have we learned from pesticide-induced animal models? *Trends in Pharmacological*
507   *Sciences.* **30** (9), 475-483 (2009).

508   13 Greenamyre, J. T., Cannon, J. R., Drolet, R., Mastroberardino, P. G. Lessons from the
509   rotenone model of Parkinson's disease. *Trends in Pharmacological Sciences.* **31** (4), 141-
510   142; author reply 142-143 (2010).

511   14 Mendes, C. S. et al. Quantification of gait parameters in freely walking rodents. *BMC*
512   *Biology.* **13**, 50 (2015).

513   15 Hamers, F. P., Lankhorst, A. J., van Laar, T. J., Veldhuis, W. B., Gispen, W. H. Automated
514   quantitative gait analysis during overground locomotion in the rat: its application to spinal
515   cord contusion and transection injuries. *Journal of Neurotrauma.* **18** (2), 187-201 (2001).

516   16 Hamers, F. P., Koopmans, G. C., Joosten, E. A. CatWalk-assisted gait analysis in the
517   assessment of spinal cord injury. *Journal of Neurotrauma.* **23** (3-4), 537-548 (2006).

518   17 Pickrell, A. M., Youle, R. J. The roles of PINK1, parkin, and mitochondrial fidelity in
519   Parkinson's disease. *Neuron.* **85** (2), 257-273 (2015).

520   18 Dawson, T. M., Ko, H. S., Dawson, V. L. Genetic animal models of Parkinson's disease.
521   *Neuron.* **66** (5), 646-661 (2010).

522   19 Gispert, S. et al. Parkinson phenotype in aged PINK1-deficient mice is accompanied by
523   progressive mitochondrial dysfunction in absence of neurodegeneration. *PLoS One.* **4** (6),
524   e5777 (2009).

525   20 Goldberg, M. S. et al. Parkin-deficient mice exhibit nigrostriatal deficits but not loss of
526   dopaminergic neurons. *Journal of Biological Chemistry.* **278** (44), 43628-43635 (2003).

527   21 Kitada, T., Tong, Y., Gautier, C. A., Shen, J. Absence of nigral degeneration in aged

528 parkin/DJ-1/PINK1 triple knockout mice. *Journal of Neurochemistry.* **111** (3), 696-702
529 (2009).
530 22 Dave, K. D. et al. Phenotypic characterization of recessive gene knockout rat models of
531 Parkinson's disease. *Neurobiology of Disease.* **70**, 190-203 (2014).
532 23 Schindelin, J. et al. Fiji: an open-source platform for biological-image analysis. *Nature*
533 *Methods.* **9** (7), 676-682 (2012).
534 24 Hruska, R. E., Kennedy, S., Silbergeld, E. K. Quantitative aspects of normal locomotion in
535 rats. *Life Sciences.* **25** (2), 171-179 (1979).
536 25 de Medinaceli, L., Freed, W. J., Wyatt, R. J. An index of the functional condition of rat
537 sciatic nerve based on measurements made from walking tracks. *Experimental Neurology.*
538 **77** (3), 634-643 (1982).
539 26 Kunkel-Bagden, E., Dai, H. N., Bregman, B. S. Methods to assess the development and
540 recovery of locomotor function after spinal cord injury in rats. *Experimental Neurology.*
541 **119** (2), 153-164 (1993).
542 27 Jacobs, B. Y., Kloefkorn, H. E., Allen, K. D. Gait Analysis Methods for Rodent Models of
543 Osteoarthritis. *Current Pain and Headache Reports.* **18** (10), 456 (2014).
544 28 Boix, J., von Hieber, D., Connor, B. Gait Analysis for Early Detection of Motor Symptoms
545 in the 6-OHDA Rat Model of Parkinson's Disease. *Frontiers in Behavioral Neuroscience.* **12**,
546 39 (2018).
547 29 Zhou, M. et al. Gait analysis in three different 6-hydroxydopamine rat models of
548 Parkinson's disease. *Neuroscience Letters.* **584**, 184-189 (2015).
549 30 Vandeputte, C. et al. Automated quantitative gait analysis in animal models of movement
550 disorders. *BMC Neuroscience.* **11**, 92 (2010).
551 31 Chuang, C. S. et al. Quantitative evaluation of motor function before and after
552 engraftment of dopaminergic neurons in a rat model of Parkinson's disease. *Journal of*
553 *Biomedical Science.* **17**, 9 (2010).
554 32 Baldwin, H. A., Koivula, P. P., Necarsulmer, J. C., Whitaker, K. W., Harvey, B. K. Step
555 Sequence Is a Critical Gait Parameter of Unilateral 6-OHDA Parkinson's Rat Models. *Cell*
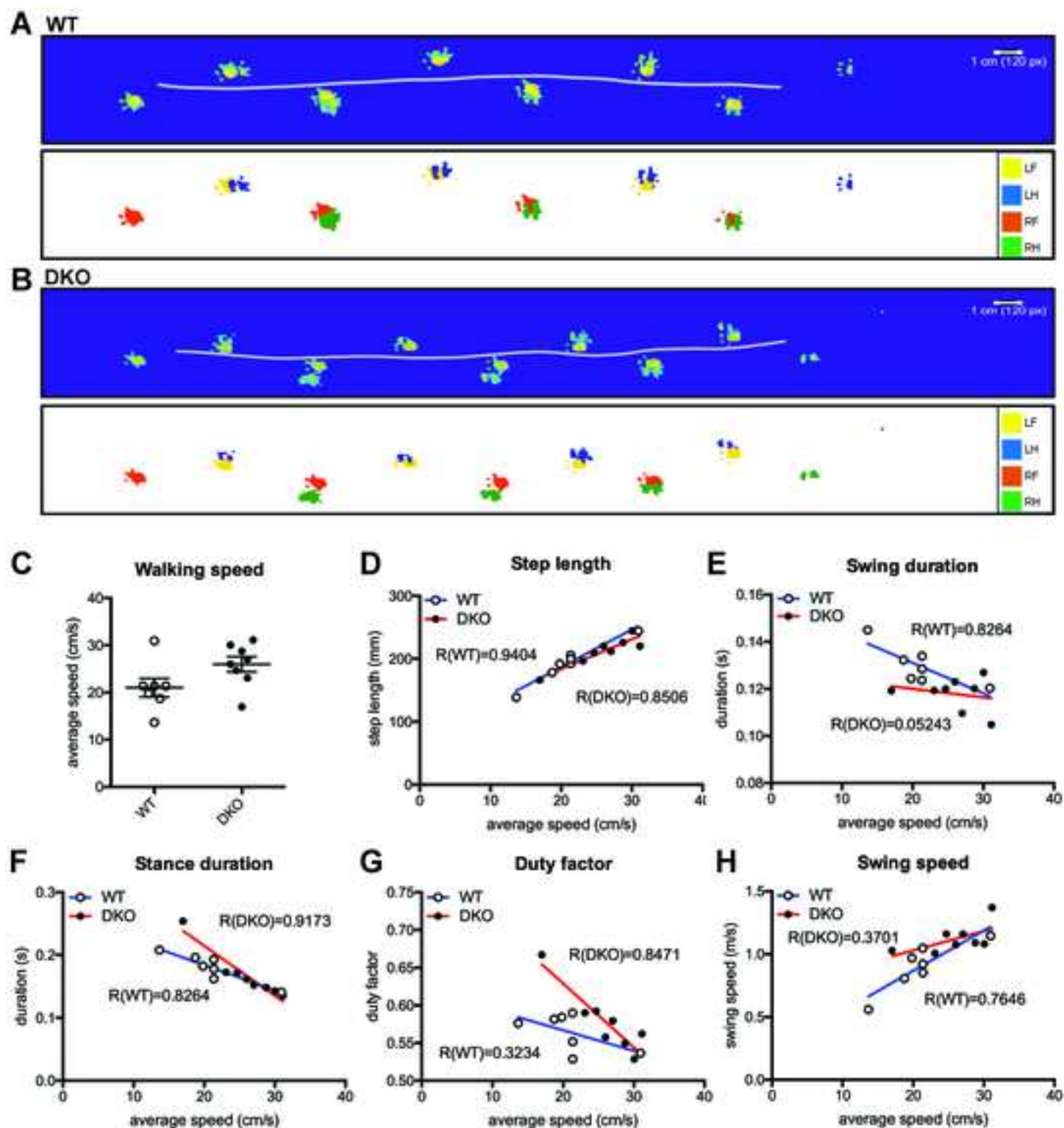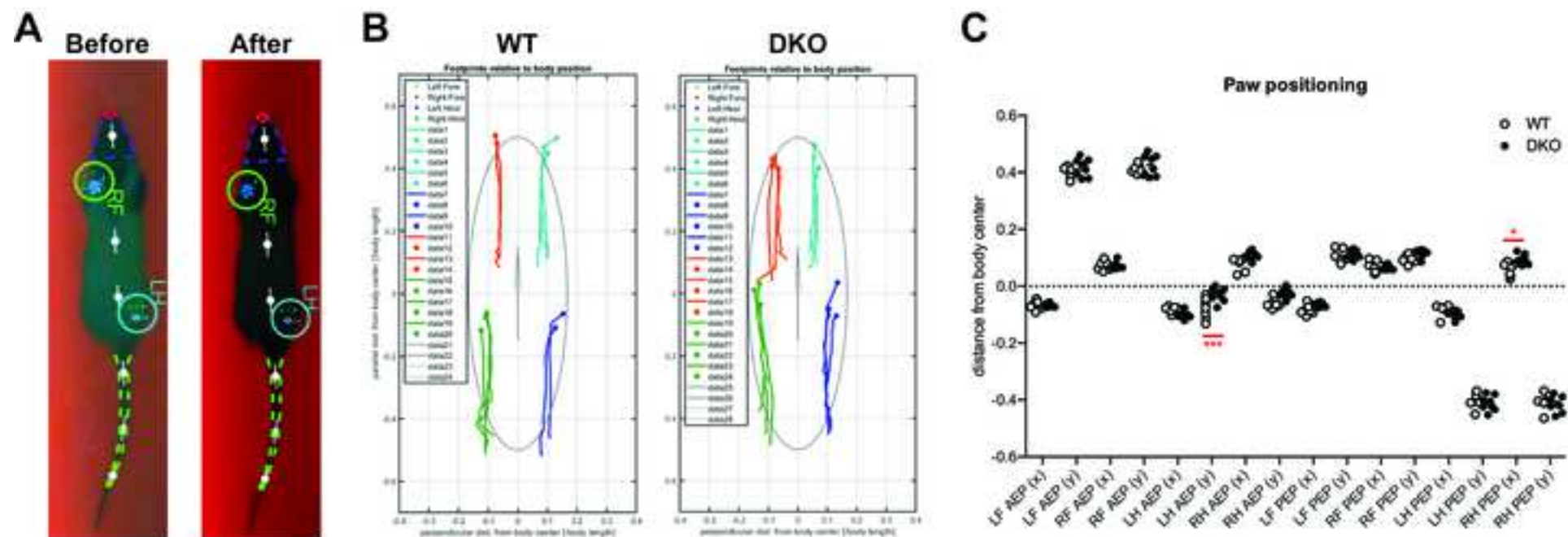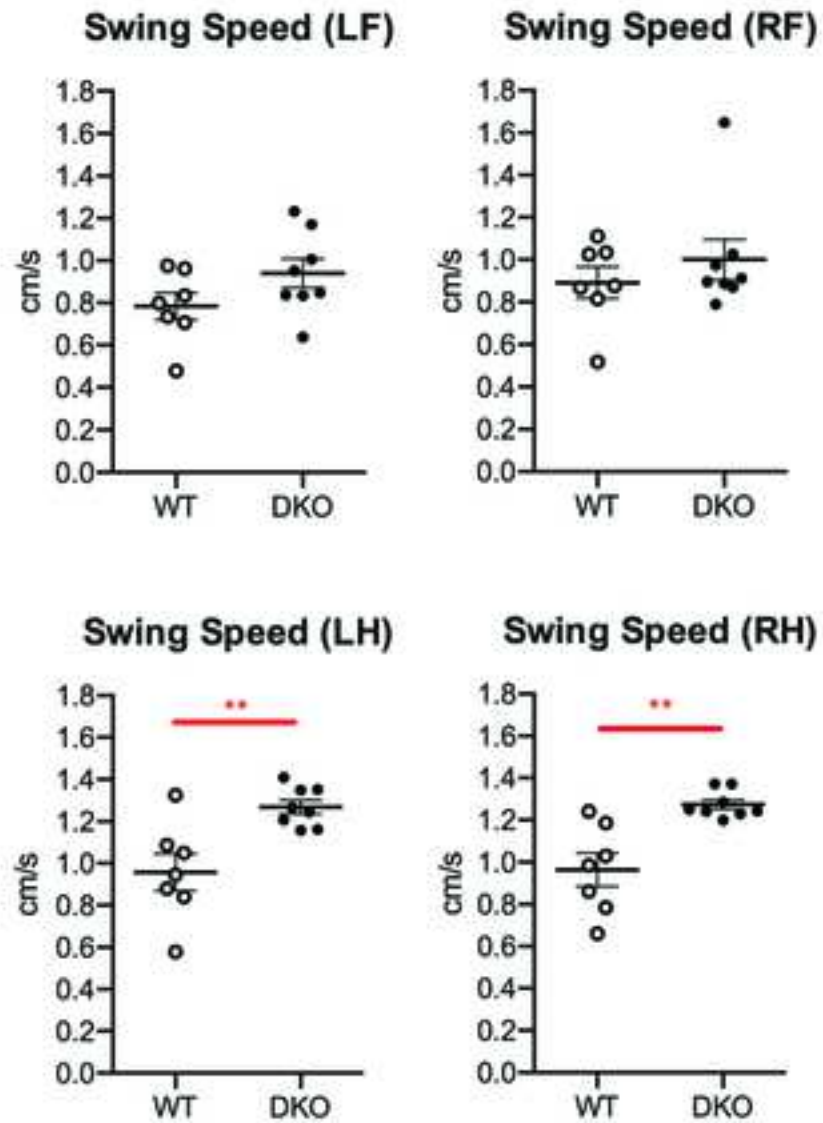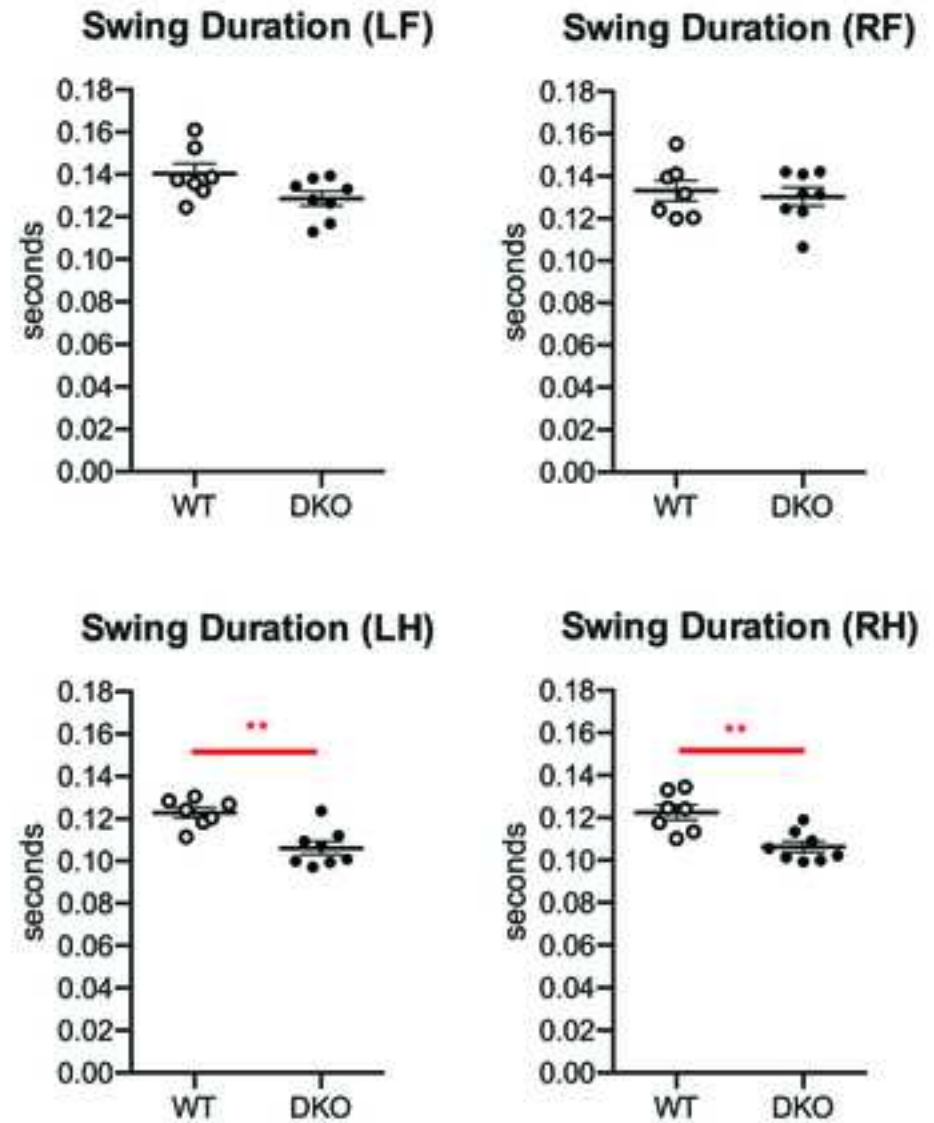556 *Transplantation.* **26** (4), 659-667 (2017).
557

Figure 1

Click here to access/download;Figure;Figure 1.tif

Figure 2

Figure 4

Click here to access/download;Figure;Figure 4.tiff

Step Length (LF)

Step Length (RF)

Step Length (LH)

Step Length (RH)
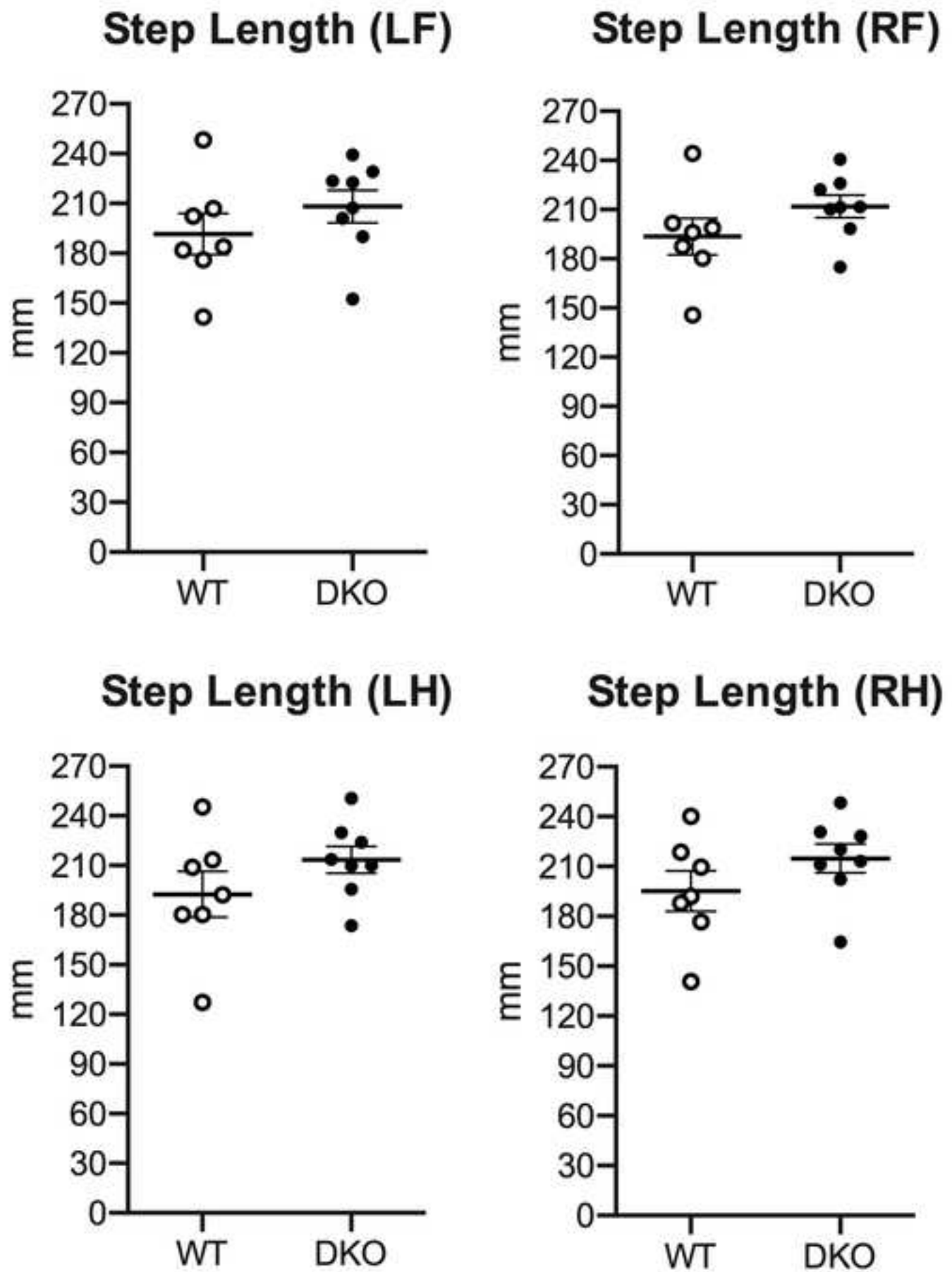
	Dimensions	Qty
Aluminum		
1.5" Aluminum Angle (1/8" - 6063)	8'	8
1" Aluminum Square Tube (1/16" - 6063)	8'	4
32 Gauge Aluminum Sheet	10'	1
1" Aluminum Tube (1/8" - 6063)	8'	1
Acrylic		
7/32" Clear Acrylic Sheet	4'x8'	2
1/8" White Acrylic Sheet 55% (2447)	4'x8'	1
Mirror		
7/32" Glass Mirror	60"x12"	1
LED		
5050 LED Tape Light (Green)	16.4'	1
5050 LED Tape Light (Red)	16.4'	1
Camera		
GoPro Hero 6 Black		1
Tripod	57"	1

Kelly L. Stauch, Ph.D.
Department of Neurological Sciences

December 21, 2020

JoVE (Journal of Visualized Experiments)
RE: JoVE62002R1 "Applying the RatWalker System for Gait Analysis in a Genetic Rat Model of Parkinson's Disease"

Dear JoVE Editors:

We would like to thank the editor for their careful review and comments regarding this manuscript resubmission. The responses to the editor's comments are provided below detailing the changes that we have made. We hope these changes make this manuscript suitable for reconsideration and publication.

Thank you for your consideration of our work.

Sincerely,

Kelly Stauch

Kelly L. Stauch, PhD, for the authors
Assistant Professor

University of Nebraska Medical Center
985800 Nebraska Medical Center
Omaha, NE 68198-5800
phone: 402 559-4552
e-mail: kelly.stauch@unmc.edu

Editorial comments:

1. There are still some scatter typos throughout the written manuscript. Please copyedit the manuscript.

The manuscript has been carefully edited to correct the typos.

2. Please highlight up to 3 pages of protocol text for inclusion in the protocol section of the video. This is a hard production limit to ensure that videography can occur in a single day.

The protocol text for inclusion in the protocol section of the video has been highlighted in yellow.

3. Additional comments are in the attached manuscript.

3a. Please revise the title for conciseness: Applying the RatWalker System for Gait Analysis in a Genetic Rat Model of Parkinson's Disease

The title has been revised accordingly.

3b. Please shorten this to 50 words or less. Please do not use references in the Summary or the Abstract.

The Summary has been shortened to less than 50 words. References have been removed from the Summary and the Abstract.

3c. Please do not cite references in the Abstract.

References have been removed from the Abstract.

3d. This is an incomplete sentence.

The incomplete sentence has been revised.

3e. leads?

The wording "does lead" has been changed to "leads".

3f. Please include an ethics statement.

An ethics statement has been added.

3g. Please move this to the introduction.

The highlighted section has been moved to the introduction.

4. Please upload the supplemental table and figures separately.

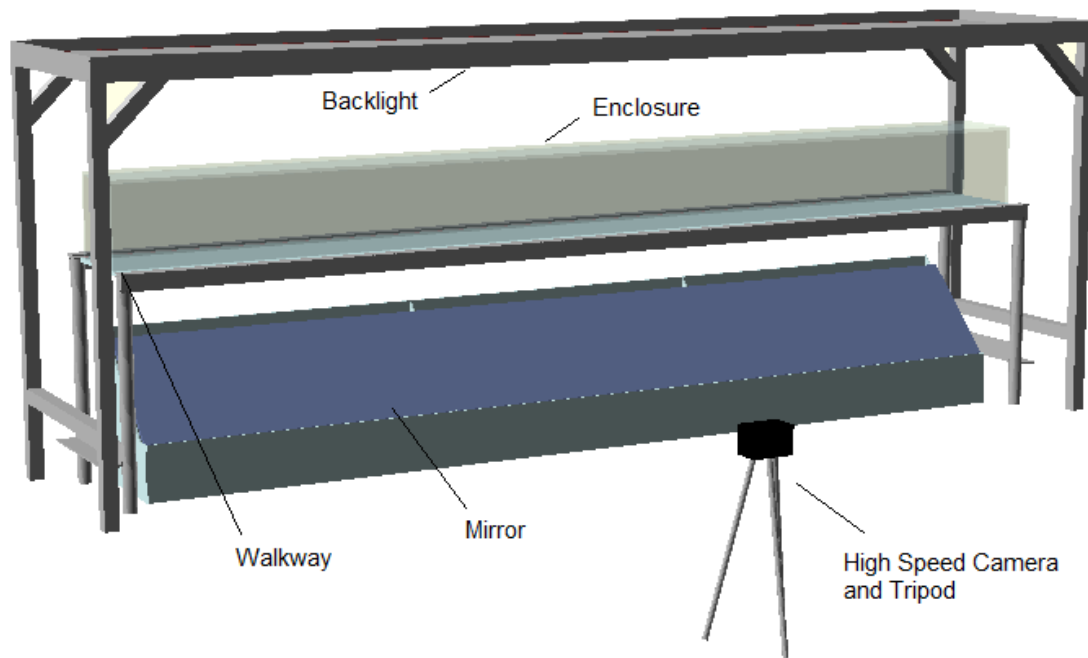*The supplemental table and figures have been uploaded separately.*
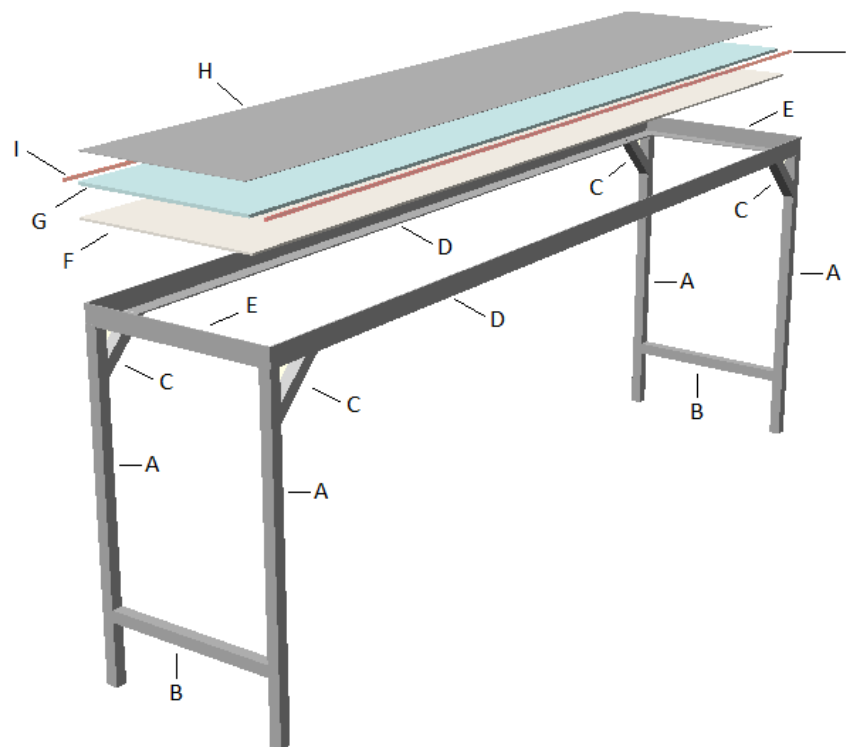
Fig S1 Rat Walker:
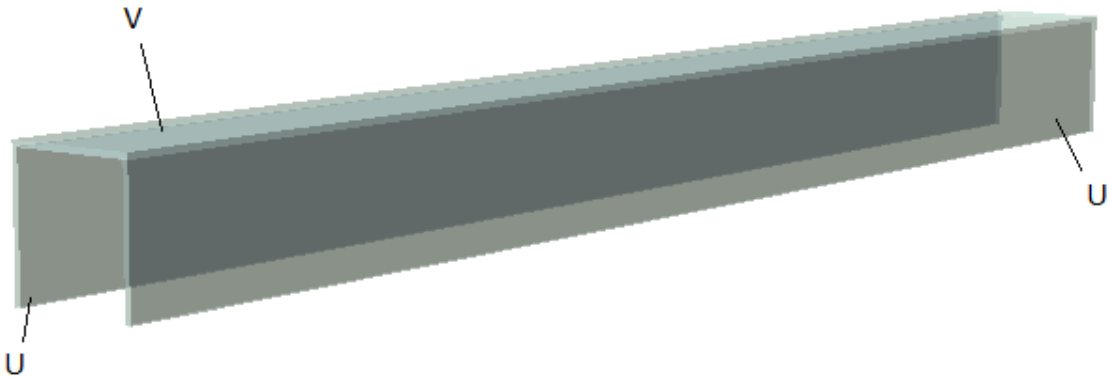

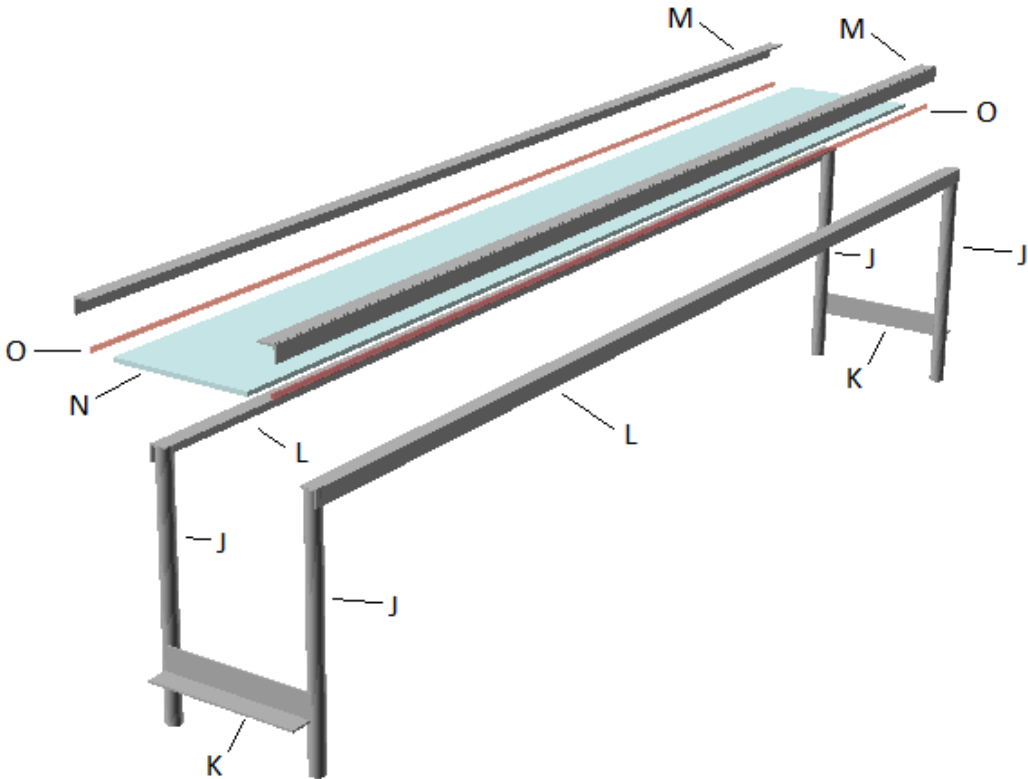Fig S2 Backlight:

Fig S3 Enclosure:

Fig S4 Walkway:

Fig S5 Mirror:
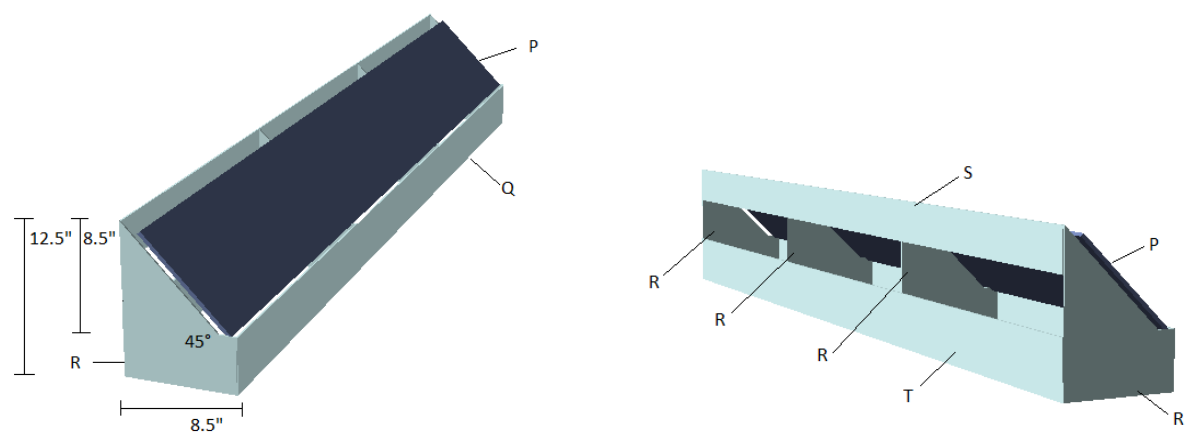

Fig S6 Software Settings

Fig S7 Genotyping

A

WT DKO

100 bp

B

CAG CCT GGG AAA CTC CGA GTT CAG TGC GGC ACC TGC AGA CAA GCA ACC CTC ACC TTG GCC CA GG TAA GGA AGC

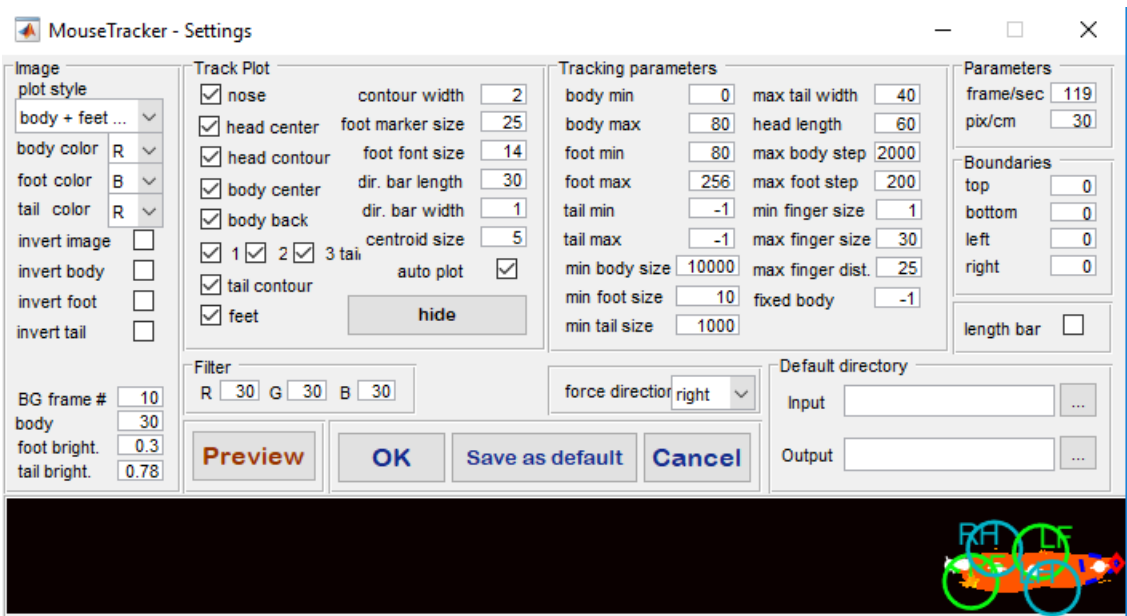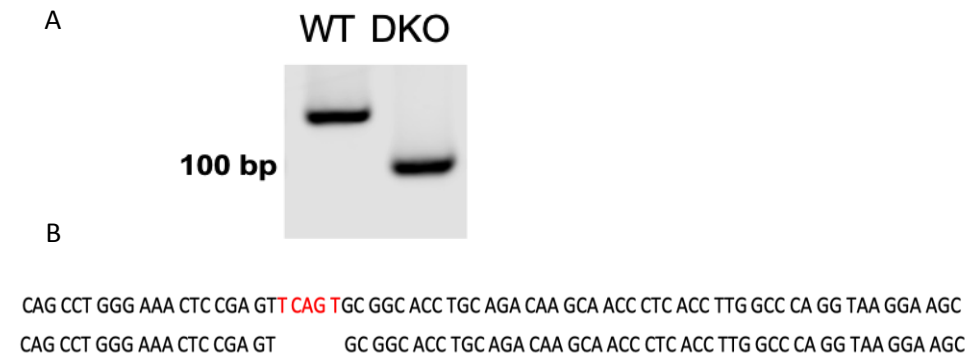CAG CCT GGG AAA CTC CGA GT   GC GGC ACC TGC AGA CAA GCA ACC CTC ACC TTG GCC CA GG TAA GGA AGC

Genotyping of DKO rats. A. Representative result of polymerase chain reaction (PCR) to confirm the deletion of 26 bp in the PINK1 in DKO rat model in comparison with WT. B. Sequencing of DKO rats to confirm the deletion of 5 bp.

Table S1				Finished Dimensions (in)		
Item ID	Item Name	Material	Qty	Length	Width	Height
A	Leg	1" Aluminum Square Tube (1/16" - 6063)	4	28.5	-	-
B	Cross Member	1" Aluminum Square Tube (1/16" - 6063)	2	14	-	-
C	Angled Support	1" Aluminum Square Tube (1/16" - 6063)	4	7	-	-
D	Side Rail	1.5" Aluminum Angle (1/8" - 6063)	2	78	-	-
E	Face Rail	1.5" Aluminum Angle (1/8" - 6063)	2	16	-	-
F	Diffusor	1/8" White Acrylic Sheet 55% (2447)	1	77.5	15.5	15.5
G	Waveguide	7/32" Clear Acrylic Sheet	1	77.5	15.5	15.5
H	Reflector	32 Gauge Aluminum Sheet	1	77.5	15.5	15.5
I	LED Light Strip	5050 LED Tape Light (Red)	1	77.5	-	-

Table S2				Finished Dimensions (in)		
Item ID	Item Name	Material	Qty	Length	Width	Height
U	Wall	7/32" Clear Acrylic Sheet	2	72	-	6
V	Ceiling	7/32" Clear Acrylic Sheet	1	72	6	-

Table S3				Finished Dimensions (in)		
Item ID	Item Name	Material	Qty	Length	Width	Height
J	Leg	1" Aluminum Tube (1/8" - 6063)	4	15	-	-
K	Cross Member	1.5" Aluminum Angle (1/8" - 6063)	2	9.5	-	-
L	Side Rail (Btm)	1.5" Aluminum Angle (1/8" - 6063)	2	72	-	-
M	Side Rail (Top)	1.5" Aluminum Angle (1/8" - 6063)	2	72	-	-
N	Walkway	7/32" Clear Acrylic Sheet	1	72	6.5	-
O	LED Light Strip	5050 LED Tape Light (Green)	1	72	-	-

Table S4				Finished Dimensions (in)		
Item ID	Item Name	Material	Qty	Length	Width	Height
P	Mirror	7/32" Glass Mirror	1	60	12	-
Q	Face Rail	7/32" Clear Acrylic Sheet	1	60	-	4.5
R	Cross Member	7/32" Clear Acrylic Sheet	1	-	8.5	12.5
S	Rear Rail (Top)	7/32" Clear Acrylic Sheet	1	60	-	3
T	Rear Rail (Btm)	7/32" Clear Acrylic Sheet	1	60	-	4